Mechanical Technology and Engineering Insights

www.mtei.reapress.com

Mech. Technol. Eng. Insights. Vol. 2, No. 3 (2025) 184–198.

Paper Type: Original Article

Free Convection of Herschel – Bulkley Fluids With MHD Effect on a Vertical Moving Plate in Porous Media

Seyed Ali Noorkhah[1,*], Natalja Osintsev[2]

[1] Department of Civil Engineering, Science and Research Branch, Islamic Azad University, 1477893855 Tehran, Iran; a.noourkhah@aihe.ac.ir.

[2] Fraunhofer-Institut für Holzforschung Wilhelm-Klauditz Institut WKI, Bienroder Weg 54 E, 38108 Brunswick, Germany; n.osintsev@gmail.com.

Citation:

Received: 14 December 2024 *Revised: 17 February 2025* *Accepted: 21 April 2025*	Noorkhah, S. A., & Osintsev, N. (2025). Free convection of Herschel–Bulkley fluids with MHD effect on a vertical moving plate in porous media. *Mechanical Technology and Engineering Insights, 2*(3), 184-198.

Abstract

In this study, a numerical investigation is carried out to analyze free convection heat transfer of a non-Newtonian Herschel–Bulkley fluid over a vertical moving plate embedded in a porous medium in the presence of a transverse magnetic field. The flow is assumed to be steady, laminar, incompressible, and electrically conducting. The governing continuity, momentum, and energy equations are formulated under the boundary layer approximation and transformed into a set of coupled, nonlinear, dimensionless equations. These equations are solved numerically using a fully implicit finite difference method. The effects of key physical parameters, including the magnetic parameter, porous medium parameter, Prandtl number, Brinkman number, Grashof number, and flow behavior index, on the transient velocity and temperature distributions are examined. In addition, the variation of the local Nusselt number is presented to characterize the heat transfer behavior. The results reveal that applying a magnetic field significantly reduces the fluid velocity while increasing the temperature, due to the Lorentz force. Increasing the porous medium parameter reduces the velocity field and increases the temperature distribution. Higher Prandtl numbers lead to thinner thermal boundary layers, resulting in reduced temperature profiles. Moreover, increasing the Brinkman number intensifies viscous dissipation, thereby increasing both velocity and temperature. The local Nusselt number decreases with increasing magnetic and Brinkman parameters, whereas it increases with higher Prandtl and Grashof numbers. The present study provides useful insight into the heat transfer characteristics of Herschel–Bulkley fluids in porous media under magnetic field effects, which are relevant to various industrial and engineering applications.

Keywords: Free convection, Herschel–Bulkley fluid, Porous medium, Vertical moving plate, Magnetohydrodynamics.

1 | Introduction

A wide range of industrially important fluids, including molten plastics, polymers, pulps, and food products, exhibit non-Newtonian fluid behavior. Due to the increasing use of these materials across various

Corresponding Author: a.noourkhah@aihe.ac.ir

https://doi.org/10.48313/mtei.v2i3.49

manufacturing and processing industries, considerable research has been devoted to understanding their flow and heat transfer characteristics. In recent years, non-Newtonian fluids have been recognized as more suitable than Newtonian fluids for many technical and engineering applications, including food processing, metallurgical operations, petroleum extraction, drilling processes, and bioengineering systems [1]. Typical examples of such fluids include clay, mud, ketchup, blood, honey, paints, slurries, molten chocolate, egg whites, and mayonnaise, whose viscosity depends on the applied shear stress.

Owing to the complex rheological behavior of non-Newtonian fluids, no single constitutive model can accurately describe all their physical characteristics. Consequently, several rheological models have been proposed, such as the power-law model [2], [3], the Jeffrey fluid model [4], the Maxwell fluid model [5], and various viscoplastic fluid models. Among these, viscoplastic fluids have attracted significant attention due to their practical relevance in industrial applications. These fluids behave as rigid solids below a critical stress, known as the yield stress, and flow as viscous fluids only when this threshold is exceeded.

Common rheological models used to describe viscoplastic fluids include the Bingham model [6], Herschel–Bulkley model [7], and Casson model [8]. Among them, the Herschel–Bulkley and Casson models are widely employed since many industrial fluids exhibit shear-thinning behavior. In particular, the Casson fluid model is extensively used in the food industry, especially in cocoa and chocolate manufacturing, and has also been adopted to describe the rheological behavior of human blood [9–12]. Numerous studies have analyzed Casson fluid flow in different geometries and under various physical conditions [13–20].

The study of non-Newtonian fluid flow and heat transfer in porous media has gained increasing attention due to its relevance in geothermal systems, chemical reactors, filtration processes, and thermal insulation technologies. Pop and Na [21] investigated free convection heat transfer of non-Newtonian fluids along a vertical wavy surface in a porous medium. Yue-Tzu and Wang [22] analyzed natural convection of a power-law fluid, with and without yield stress, around a two-dimensional axisymmetric body in a fluid-saturated porous medium. Similarity solutions for natural convection of non-Newtonian fluids over vertical surfaces in porous media were presented by Chen and Chen [23]. Jumah and Mujumder [24] examined coupled heat and mass transfer in free convection flow of Herschel–Bulkley fluids over a vertical flat plate embedded in a porous medium. Abel and Veena [25] studied the effects of viscoelasticity on flow and heat transfer over a stretching sheet in a porous medium. At the same time, Bestman [26] investigated the natural convection boundary-layer flow with suction and mass transfer in porous media.

Despite these efforts, comparatively fewer studies have addressed non-Newtonian fluid flow in porous media, as highlighted by Shenoy [27]. The interaction of magnetic fields with convective heat transfer in porous media has further expanded research interest due to its applications in Magnetohydrodynamics (MHD), generators, cooling of nuclear reactors, and electromagnetic flow control. Makinde [28] investigated transient free convection with thermal radiation along a moving vertical permeable plate. Chamkha [29] analyzed MHD flow past a moving plate embedded in a porous medium under a transverse magnetic field. At the same time, Kim [30] studied unsteady MHD convective heat transfer past a semi-infinite vertical porous moving plate. Group-theoretical analyses of unsteady free-convection MHD flows in porous media were presented by El-Hakiem et al. [31] and Abd El-Naby et al. [32]. Ganesan and Palani [33] provided a numerical solution for transient MHD free convection flow past an inclined plate, considering variable heat and mass fluxes.

Further investigations include the work of Makinde [28] on transient free convection with radiation effects, and Mahesh Kumari and Girishwar Nath [34], who studied conjugate mixed convection heat transfer of power-law fluids over a moving vertical heated plate. El-Hakiem et al. [31] extended their analysis to unsteady MHD free convection flows in fluid-saturated porous media. Cheng and Lee [35] examined free-convection heat transfer in micropolar fluids under thermal stratification conditions.

Motivated by the above studies and the limited literature on Herschel–Bulkley fluids under combined porous medium and magnetic field effects, the present work investigates the steady laminar heat transfer of an incompressible, electrically conducting Herschel–Bulkley non-Newtonian fluid flowing past a two-dimensional vertical moving plate embedded in a porous medium in the presence of a uniform transverse

magnetic field. The governing continuity, momentum, and energy equations are solved numerically using an implicit finite difference method. The effects of key parameters, including the Prandtl number, Brinkman number, flow behavior index, porous medium parameter, Grashof number, and magnetic parameter, on the velocity and temperature fields are analyzed. In addition, the local Nusselt number is evaluated and presented graphically.

2 | Mathematical Formulation

The Physical model, coordinate system, and boundary conditions are shown in *Fig. 1*. Consider an MHD free convection flow of an electrically conducting fluid for Non-Newtonian Herschel-Bulkley fluids with porous medium over an isothermal vertical moving plate. The x-axis is assumed to be taken along the plate, and the y-axis is normal to the plate. The wall is maintained at constant temperature T_w and then the ambient temperature T_∞ respectively. A uniform magnetic field is applied normal to the plate with magnitude B0.

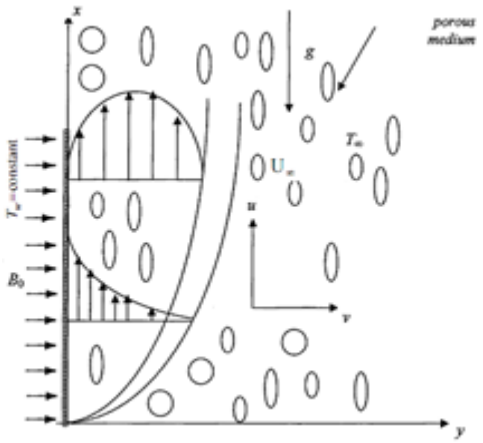

Fig. 1. Physical model and coordinate system.

The governing equations include mass conservation in a continuous medium (*Eq. (1)*), the Navier-Stokes equation (*Eq. (2)*), and the energy equation (*Eq. (3)*).

$$\frac{\partial u}{\partial x}+\frac{\partial v}{\partial y}=0, \tag{1}$$

$$\frac{\partial u}{\partial t}+u\frac{\partial u}{\partial x}+v\frac{\partial u}{\partial y}=\frac{1}{\rho}\frac{\partial}{\partial y}\left[\mu\frac{\partial u}{\partial y}\right]+g\beta\left(T-T_\infty\right)-\left(\frac{\upsilon_L}{\rho k}+\frac{\sigma B_0^2}{\rho}\right)u. \tag{2}$$

$$\frac{\partial T}{\partial t}+u\frac{\partial T}{\partial x}+v\frac{\partial T}{\partial y}=\alpha\frac{\partial^2 T}{\partial y^2}+\phi_1+\phi_2. \tag{3}$$

$$\phi_1=\mu\left(\frac{\partial u}{\partial y}\right)^2. \tag{4}$$

$$\phi_2=(MN)u^2. \tag{5}$$

The non-Newtonian fluid model used in this study is the Herschel-Bulkley model (*Eq. (6)*.

$$\tau=\tau_Y+m\left|\frac{\partial u}{\partial y}\right|^N. \tag{6}$$

The Coefficient of dynamic viscosity, μ, for Herschel–Bulkley fluids is given by *Eq. (7)*.

$$\mu = \frac{\tau_Y}{\left|\frac{\partial u}{\partial y}\right|} + m\left|\frac{\partial u}{\partial y}\right|^{N-1}. \tag{7}$$

The physical problem is assumed to satisfy the following initial and boundary conditions (*Eq. (8)*.

$$\begin{aligned} &t \le 0,\ v = 0,\ \ u = 0,\ \ T = T_\infty, \\ &t > 0,\ u = u_P,\ \ v = 0,\ T = T_w, \text{ at } \quad y = 0,\ u = 0. \\ &x{=}0, T = T_\infty \quad u \to 0, \text{ at } y \to 0,\ T \to T_\infty,\ u \to 0. \end{aligned} \tag{8}$$

Introducing the following dimensionless quantities, *Eq. (9)*:

$$\begin{aligned} &X = \frac{xu_P}{\upsilon_L},\ Y = \frac{yu_P}{\upsilon_L},\ U = \frac{u}{u_P},\ V = \frac{v}{u_P}, \\ &t' = \frac{tu_P^2}{\upsilon_L},\ \theta = \frac{T - T_\infty}{T_w - T_\infty},\ MN = \frac{\upsilon_L \sigma B_0^2}{\rho u_P^2} \\ &Gr = \frac{\upsilon_L g\beta(T_w - T_\infty)}{u_P^3},\ NU = \frac{hX}{k},\ Pr = \frac{\upsilon_L}{\alpha}, \\ &K_P = \frac{\upsilon_L^2}{\rho k u_P^2},\ \bar{\mu} = \frac{\mu}{\mu_L},\ \bar{\mu} = \frac{\bar{\tau}_Y}{\left|\frac{\partial U}{\partial Y}\right|} + \left|\frac{\partial U}{\partial Y}\right|^{N-1} \\ &\mu_L = m\left(\frac{u_P^2}{\upsilon_L}\right)^{N-1}, \bar{\tau}_Y = \frac{\tau_Y}{\rho u_P^2}, Br = \frac{\mu_L u_P^2}{k\left(T_W - T_\infty\right)}. \end{aligned} \tag{9}$$

The governing equations can be rewritten in dimensionless form as follows:

$$\begin{aligned} &\frac{\partial U}{\partial X} + \frac{\partial V}{\partial Y} = 0, \\ &\frac{\partial U}{\partial t'} + U\frac{\partial U}{\partial X} + V\frac{\partial U}{\partial Y} = N\frac{\partial^2 U}{\partial Y^2}\left|\frac{\partial U}{\partial Y}\right|^{N-1}. \end{aligned} \tag{10}$$

$$+Gr\theta - \left(K_P + MN\right)U \frac{\partial \theta}{\partial t'} + U\frac{\partial \theta}{\partial X} + V\frac{\partial \theta}{\partial Y} = \tag{11}$$

$$\frac{1}{Pr}\frac{\partial^2 \theta}{\partial Y^2} + \bar{\phi}_1 + \bar{\phi}_2. \tag{12}$$

$$\bar{\phi}_1 = \frac{Br}{Pr}\left|\frac{\partial U}{\partial Y}\right|^{N+1} + \frac{Br\bar{\tau}_Y}{Pr}\left|\frac{\partial U}{\partial Y}\right|. \tag{13}$$

$$\bar{\phi}_2 = \frac{Br}{Pr}MNU^2. \tag{14}$$

The corresponding initial and boundary conditions in non-dimensional form are given by *Eq. (15)*.

$$t' \le 0,\ \theta = 0,\ V = 0,\ U = 0,$$
$$t' > 0,\ U = 1,\ U = 0,\ Y = 0,\ \text{ta}\ \ \theta = 1,\ V = 0, \tag{14}$$

$$X=0,\ \theta = 0,\ U \to 0,\ \theta = 0,\quad \text{at}\quad Y \to 0. \tag{15}$$

The local as well as Nusselt number in terms of dimensionless quantities are given by:

$$NU = -X\frac{\partial \theta}{\partial Y}\Big|_{Y=0}. \tag{15}$$

3 | Results and Discussions

The transformed governing *Eqs. (10)-(12)* and the associated initial and boundary *Conditions (15)* can be solved by the implicit finite difference method. In the paper, we focused on the effects of the magnetic field parameter, porous medium parameter, Prandtl number, Brinkman number, Grashof number, and flow behavior index on the transient velocity, temperature, and concentration profiles, as well as on the local heat.

Figs .2 and *3* describe the behavior of transient velocity and temperature with changes in the values of X. It is observed that the velocity and temperature increase with increasing X.

Figs. 4 and *5* show the effect of the magnetic field parameter MN on the velocity and temperature profile. It is observed that the velocity decreases with increases in MN parameters. However, the Temperature increases with increasing MN parameters.

Fig. 6 and *7* describe the behavior of transient velocity and temperature for fluids with different values of power-law index N. It can be observed that the temperature decreases monotonically with increasing N, whereas the velocity exhibits different behavior for small and large N.

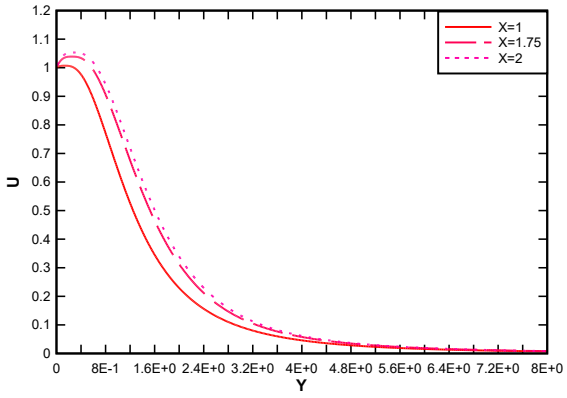

Fig. 2. Comparison of velocity profiles at different values of X, MN=1, Pr=10, K_P=0.2, τ_D=0.6 , Gr =5 , Br=0.5

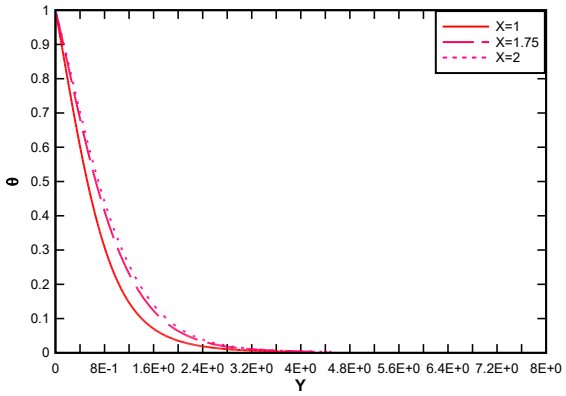

Fig. 3. Comparison of temperature profiles at different values of X, MN=1, Pr=10, K_P=0.2, τ_D=0.6 , Gr =5 , Br=0.5.

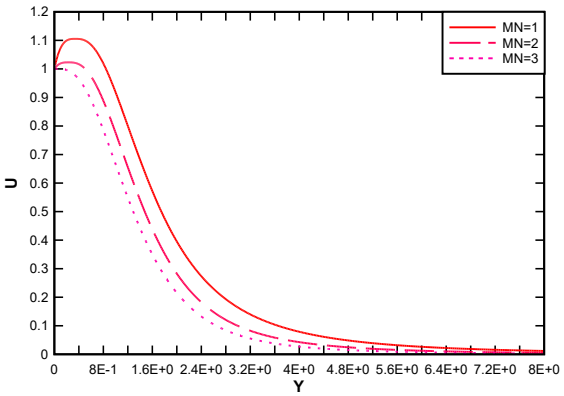

Fig. 4. Transient velocity profiles for the different values of parameter M and for the values X=2, Pr=10, N=1.5,$\bar{\tau}_Y$=0.6 , Kp=0.2 , Br=0.5 ,GR=5.

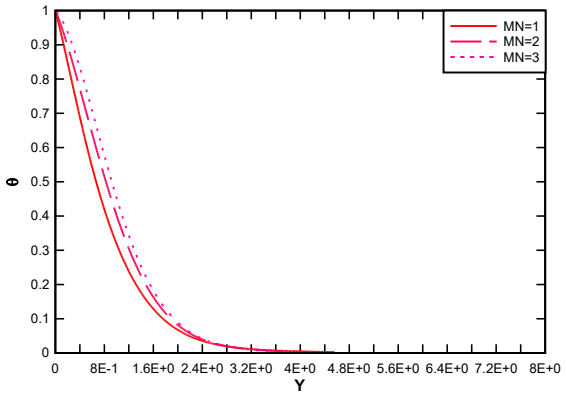

Fig. 5. Transient temperature profiles for the different values of parameter M and for the values X=2, Pr=10, N=1.5, $\bar{\tau}_Y$=0.6, Kp=0.2, Br=0.5, GR=5.

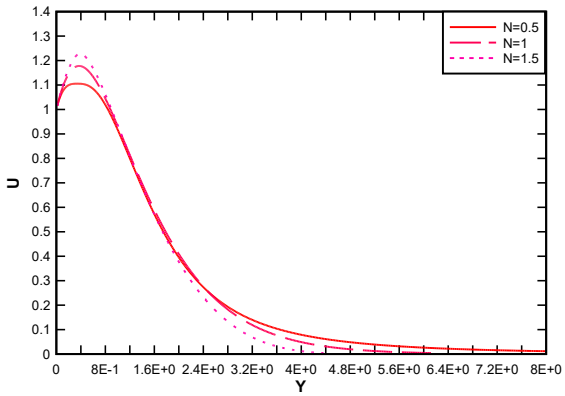

Fig. 6. Transient velocity profiles for the different values of parameter N and for the values X=2, Pr=10, $\bar{\tau}_Y$ =0.6, Kp=0.2, M=1, Br=0.5, GR=5.

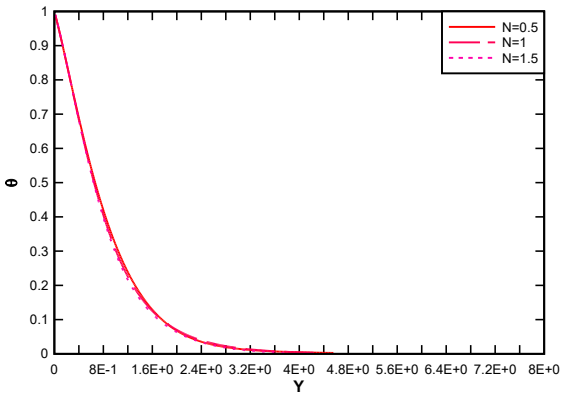

Fig. 7. Transient temperature profiles for the different values of parameter N and for the values X=2, Pr=10, $\bar{\tau}_Y$=0.6, Kp=0.2, M=1, Br=0.5, GR=5.

Figs. 8 and *9* show the effect of the porous medium parameter Kp on the Velocity and temperature profiles. It is observed that the velocity decreases with increasing Kp parameters. However, the Temperature increases with increasing Kp parameters.

Figs. 10 and *11* show the effect of the Grashof number on transient velocity and temperature distribution. It is observed that the velocity increases with increasing Grashof number. However, the Temperature decreases with increasing Grashof number.

Figs. 12 and *13* show the effect of the Prandtl number on the transient velocity and temperature distributions. Both velocity and temperature decrease as the Prandtl number increases. It agrees with the physical fact that the thermal boundary layer thickness decreases with increasing Prandtl number.

Figs. 14 and *15* show the effect of Brinkman number on transient velocity and temperature distribution. Both velocity and temperature increase as the Brinkman number increases.

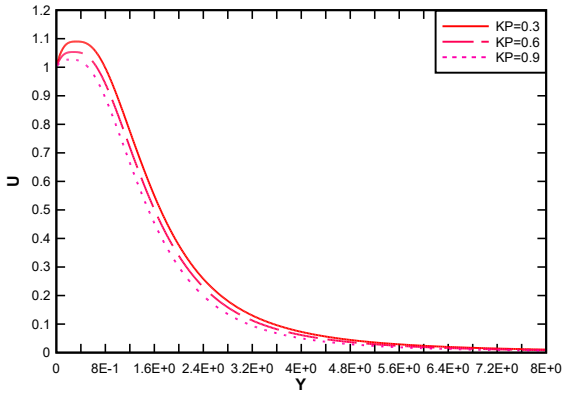

Fig. 8. Transient velocity profiles for the different values of parameter Kp and for the values X=2, Pr=10, N=1.5, $\bar{\tau}_Y$=0.6, M=1, Br=0.5, GR=5.

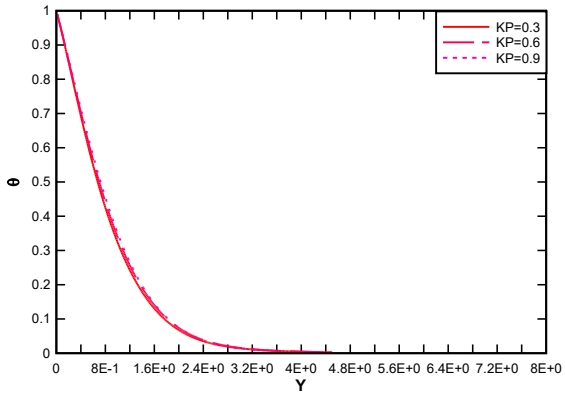

Fig. 9. Transient temperature profiles for the different values of parameter Kp and for the values X=2, Pr=10, N=1.5, $\bar{\tau}_Y$=0.6, M=1, Br=0.5, GR=5.

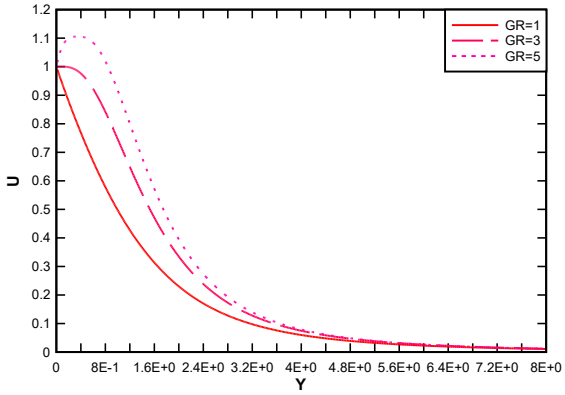

Fig. 10. Transient velocity profiles for the different values of parameter GR and for the values X=2, Pr=10, N=1.5, $\bar{\tau}_Y$=0.6, M=1, Kp=0.2, Br=0.5.

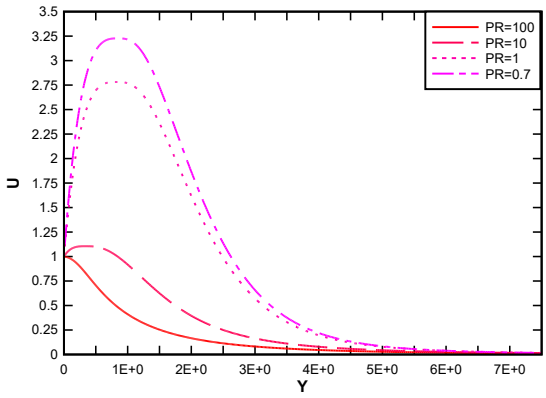

Fig. 11. Transient temperature profiles for the different values of parameter GR and for the values X=2, Pr=10, N=1.5,$\bar{\tau}_Y$=0.6, M=1, Kp=0.2, Br=0.5.

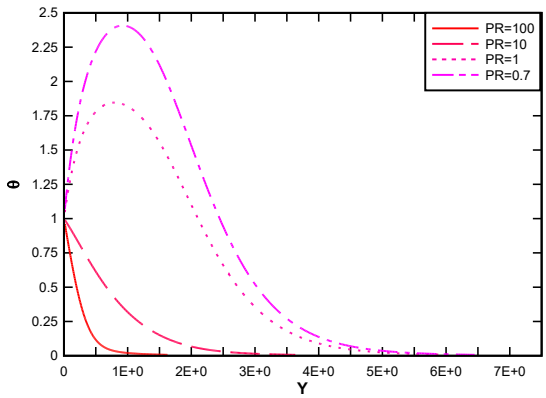

Fig. 12. Transient velocity profiles for the different values of parameter Pr and for the values X=2, N=1.5, $\bar{\tau}_Y$=0.6 M=1, Kp=0.2, Br=0.5, GR=5.

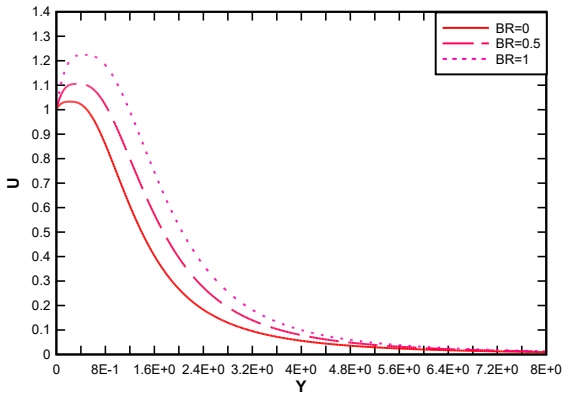

Fig. 13. Transient temperature profiles for the different values of parameter Pr and for the values X=2, N=1.5, $\bar{\tau}_Y$=0.6 M=1, Kp=0.2, Br=0.5, GR=5.

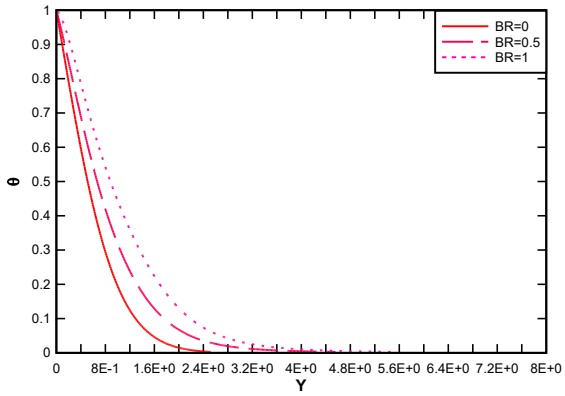

Fig. 14. Transient velocity profiles for the different values of parameter BR and for the values X=2, N=1.5,$\bar{\tau}_Y$=0.6, M=1 , Kp=0.2 , Pr=10 , GR=5.

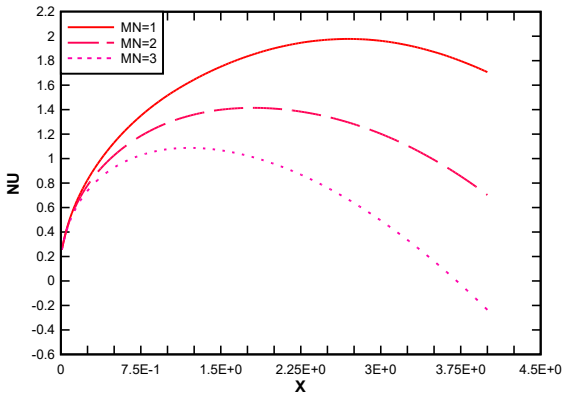

Fig. 15. Transient temperature profiles for the different values of parameter BR and for the values X=2, N=1.5, $\bar{\tau}_Y$=0.6, M=1, Kp=0.2, Pr=10, GR=5.

Fig. 16 shows the effect of the MN parameter on the local Nusselt number respectively. It is observed that the local Nusselt number decreases as MN increases.

Fig. 17 shows the effect of the Brinkman number on the local Nusselt number. It is observed that the local Nusselt number decreases with increasing Brinkman number.

Fig. 18 shows the effect of the Prandtl number on the local Nusselt number. It is observed that the local Nusselt number increases with increasing Prandtl number.

Fig. 19 shows the effect of the Grashof number on the local Nusselt number respectively. It is observed that the local Nusselt number increases with increasing Grashof number.

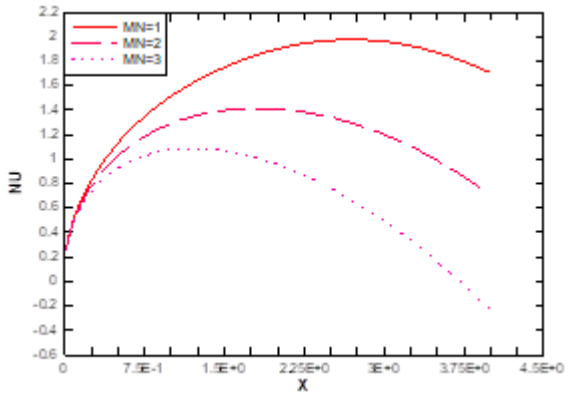

Fig. 16. The effect of MN parameter on the local Nusselt number at X=2, Pr=10, N=1.5,$\bar{\tau}_Y$=0.6, Kp=0.2, Br=0.5, GR=5.

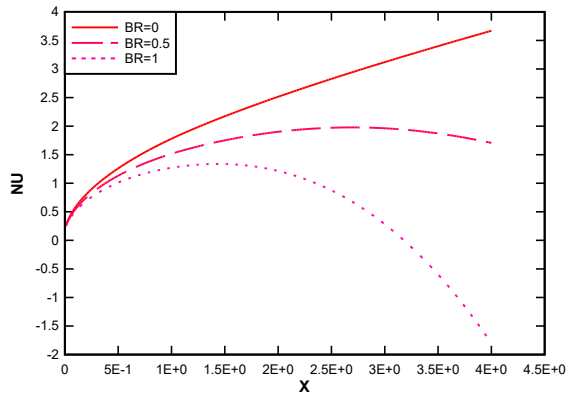

Fig. 17. The effect of the BR parameter on the local Nusselt number at X=2, Pr=10, N=1.5, $\bar{\tau}_Y$=0.6, Kp=0.2, GR=5.

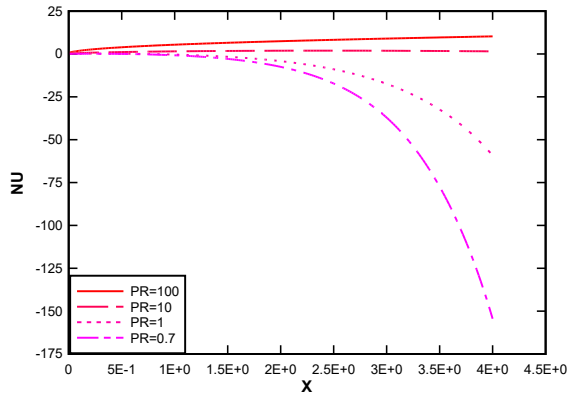

Fig. 18. The effect of PR parameter on the local Nusselt number at X=2, N=1.5, M=1,$\bar{\tau}_Y$=0.6, Kp=0.2, Br=0.5, GR=5.

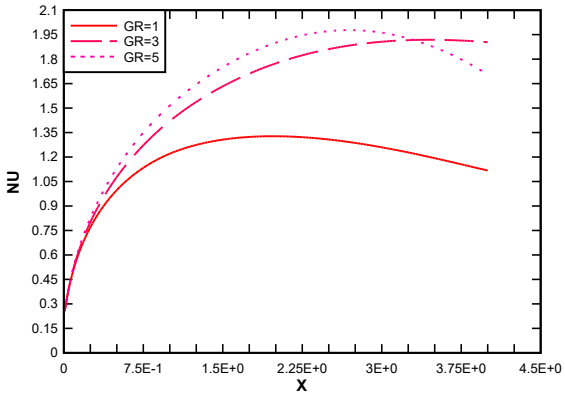

Fig. 19. The effect of GR parameter on the local Nusselt number at X=2, Pr=10, N=1.5, $\bar{\tau}_Y$=0.6, M=1, Kp=0.2, Br=0.5.

4 | Conclusion

A numerical study has been performed to investigate free-convection heat transfer of a Herschel–Bulkley non-Newtonian fluid over a vertical moving plate embedded in a porous medium, under the influence of a transverse magnetic field. The governing boundary-layer equations were solved using an implicit finite-difference method, and the effects of various governing parameters on velocity, temperature, and local heat transfer characteristics were analyzed in detail.

The results demonstrate that the magnetic field parameter exerts a pronounced damping effect on the fluid velocity through the Lorentz force. At the same time, it enhances the temperature distribution within the boundary layer. Increasing the porous medium parameter leads to greater resistance to the flow, resulting in reduced velocity and increased temperature profiles. The Prandtl number plays a significant role in controlling the thermal boundary layer thickness, with higher Prandtl numbers producing lower temperature distributions and enhanced heat transfer rates. The Brinkman number strongly affects the flow behavior through viscous dissipation, causing both velocity and temperature to increase as its value rises. Furthermore, the buoyancy force represented by the Grashof number significantly enhances fluid motion and heat transfer. The local Nusselt number decreases with increasing magnetic and Brinkman parameters.

In contrast, it increases with higher Prandtl and Grashof numbers, indicating improved heat transfer performance under strong buoyancy effects and reduced viscous dissipation. Overall, the present analysis provides a comprehensive understanding of the combined effects of non-Newtonian fluid behavior, porous media resistance, and magnetic fields on free convection heat transfer. The findings of this study may be useful in the design and optimization of thermal systems involving electrically conducting non-Newtonian fluids, such as polymer processing, geothermal systems, and MHD-based heat transfer devices.

Conflict of Interest

The authors declare no conflict of interest.

Data Availability

All data are included in the text.

Funding

This research received no specific grant from funding agencies in the public, commercial, or not-for-profit sectors.

References

[1] Ghigo, A. R., Lagrée, P. Y., & Fullana, J. M. (2018). A time-dependent non-Newtonian extension of a 1D blood flow model. *Journal of non-newtonian fluid mechanics*, *253*, 36–49. https://doi.org/10.1016/j.jnnfm.2018.01.004

[2] Chandra, A., & Chhabra, R. P. (2011). Influence of power-law index on transitional Reynolds numbers for flow over a semi-circular cylinder. *Applied mathematical modelling*, *35*(12), 5766–5785. https://doi.org/10.1016/j.apm.2011.05.004

[3] Chandra, A., & Chhabra, R. P. (2012). Laminar free convection from a horizontal semi-circular cylinder to power-law fluids. *International journal of heat and mass transfer*, *55*(11), 2934–2944. https://doi.org/10.1016/j.ijheatmasstransfer.2012.02.034

[4] Santhosh, N., Radhakrishnamacharya, G., & Chamkha, A. J. (2015). Flow of a Jeffrey fluid through a porous medium in narrow tubes. *Journal of porous media*, *18*(1), 71–78. https://alichamkha.net/wp-content/uploads/2022/14/386.pdf

[5] Aman, S., Al-Mdallal, Q., & Khan, I. (2020). Heat transfer and second order slip effect on MHD flow of fractional Maxwell fluid in a porous medium. *Journal of King Saud university-science*, *32*(1), 450–458. https://doi.org/10.1016/j.jksus.2018.07.007

[6] Bingham, E. (1916). The behavior of plastic materials. *Bulletin of us bureau of standards*, *13*, 309–353.

[7] Herschel, W. H. (1924). Consistency of rubber benzene solutions. *Industrial & engineering chemistry*, *16*(9), 927. https://doi.org/10.1021/ie50177a019

[8] Casson, N. (1959). Flow equation for pigment-oil suspensions of the printing ink-type. *Rheology of disperse systems*, 84–104. https://cir.nii.ac.jp/crid/1571980076287959296

[9] Mandal, P. K. (2004). Unsteady flow of a two-layer blood stream past a tapered flexible artery under stenotic conditions. *Computational methods in applied mathematics*, *4*(4), 391–409. https://doi.org/10.2478/CMAM-2004-0022

[10] Tzirakis, K., Botti, L., Vavourakis, V., & Papaharilaou, Y. (2016). Numerical modeling of non-Newtonian biomagnetic fluid flow. *Computers & fluids*, *126*, 170–180. https://doi.org/10.1016/j.compfluid.2015.11.016

[11] Sankar, D. S., & Lee, U. (2010). Two-fluid Casson model for pulsatile blood flow through stenosed arteries: A theoretical model. *Communications in nonlinear science and numerical simulation*, *15*(8), 2086–2097. https://doi.org/10.1016/j.cnsns.2009.08.021

[12] Boyd, J., Buick, J. M., & Green, S. (2007). Analysis of the Casson and Carreau-Yasuda non-Newtonian blood models in steady and oscillatory flows using the lattice Boltzmann method. *Physics of fluids*, *19*(9), 093103. https://doi.org/10.1063/1.2772250

[13] Abolbashari, M. H., Freidoonimehr, N., Nazari, F., & Rashidi, M. M. (2015). Analytical modeling of entropy generation for Casson nano-fluid flow induced by a stretching surface. *Advanced powder technology*, *26*(2), 542–552. https://doi.org/10.1016/j.apt.2015.01.003

[14] Mythili, D., & Sivaraj, R. (2016). Influence of higher order chemical reaction and non-uniform heat source/sink on Casson fluid flow over a vertical cone and flat plate. *Journal of molecular liquids*, *216*, 466–475. https://doi.org/10.1016/j.molliq.2016.01.072

[15] Rahman, M. M., & Pop, I. (2016). Effects of second-order slip and viscous dissipation on the analysis of the boundary layer flow and heat transfer characteristics of a Casson fluid. *Sultan qaboos university journal for science*, *21*(1), 48–63. https://doi.org/10.24200/squjs.vol21iss1pp48-63

[16] Pop, I., & Sheremet, M. (2017). Free convection in a square cavity filled with a Casson fluid under the effects of thermal radiation and viscous dissipation. *International journal of numerical methods for heat & fluid flow*, *27*(10), 2318–2332. https://doi.org/10.1108/HFF-09-2016-0352

[17] Gireesha, B. J., Archana, M., B.C., P., Gorla, R. S. R., & Makinde, O. D. (2017). MHD three dimensional double diffusive flow of Casson nanofluid with buoyancy forces and nonlinear thermal radiation over a

stretching surface. *International journal of numerical methods for heat & fluid flow*, *27*(12), 2858–2878. https://doi.org/10.1108/HFF-01-2017-0022

[18] Ullah, I., Alkanhal, T. A., Shafie, S., Nisar, K. S., Khan, I., & Makinde, O. D. (2019). MHD Slip Flow of Casson Fluid along a Nonlinear Permeable Stretching Cylinder Saturated in a Porous Medium with Chemical Reaction, Viscous Dissipation, and Heat Generation/Absorption. *Symmetry*, *11*(4), 531. https://doi.org/10.3390/sym11040531

[19] Mahanthesh, B., Gireesha, B. J., Shashikumar, N. S., Hayat, T., & Alsaedi, A. (2018). Marangoni convection in Casson liquid flow due to an infinite disk with exponential space dependent heat source and cross-diffusion effects. *Results in physics*, *9*, 78–85. https://doi.org/10.1016/j.rinp.2018.02.020

[20] Rao, A. S., Sainath, S., Rajendra, P., & Ramu, G. (2019). Mathematical modelling of hydromagnetic casson non-Newtonian nanofluid convection slip flow from an isothermal sphere. *Nonlinear engineering*, *8*(1), 645–660. 10.1515/nleng-2018-0016/html

[21] Pop, T., & Na, T. Y. (1996). *Free convection heat transfer of non-newtonian fluids along a vertical wavy surface in a porous medium* [**Presentation**]. Proceedings of the.4th international symposium on heat transfer (p. 452).

[22] Yang, Y. T., & Wang, S. J. (1996). Free convection heat transfer of non-Newtonian fluids over axisymmetric and two-dimensional bodies of arbitrary shape embedded in a fluid-saturated porous medium. *International journal of heat and mass transfer*, *39*(1), 203–210. https://doi.org/10.1016/S0017-9310(96)85016-2

[23] Chen, H. T., & Chen, C. K. (1988). Free convection flow of non-Newtonian fluids along a vertical plate embedded in a porous medium. *Journal of heat transfer (transactions of the ASME (American society of mechanical engineers), series c);(United States)*, *110*(1), 257–260. https://www.osti.gov/biblio/5981575

[24] Jumah, R. Y., & Mujumdar, A. S. (2000). Free convection heat and mass transfer of non-newtonian power law fluids with yield stress from a vertical flat plate in saturated porous media. *International communications in heat and mass transfer*, *27*(4), 485–494. https://doi.org/10.1016/S0735-1933(00)00131-7

[25] Subhas, A., & Veena, P. (1998). Visco-elastic fluid flow and heat transfer in a porous medium over a stretching sheet. *International journal of non-linear mechanics*, *33*(3), 531–540. https://doi.org/10.1016/S0020-7462(97)00025-5

[26] Bestman, A. R. (1990). Natural convection boundary layer with suction and mass transfer in a porous medium. *International journal of energy research*, *14*(4), 389–396. https://doi.org/10.1002/er.4440140403

[27] Shenoy, A. V. (1994). Non-newtonian fluid heat transfer in porous media. In advances in heat transfer, *Advances in heat transfer* (Vol. 24, pp. 101–190). Elsevier. https://doi.org/10.1016/S0065-2717(08)70233-8

[28] Makinde, O. D. (2005). Free convection flow with thermal radiation and mass transfer past a moving vertical porous plate. *International communications in heat and mass transfer*, *32*(10), 1411–1419. https://doi.org/10.1016/j.icheatmasstransfer.2005.07.005

[29] Chamkha, A. J. (2004). Unsteady MHD convective heat and mass transfer past a semi-infinite vertical permeable moving plate with heat absorption. *International journal of engineering science*, *42*(2), 217–230. https://doi.org/10.1016/S0020-7225(03)00285-4

[30] Kim, Y. J. (2000). Unsteady MHD convective heat transfer past a semi-infinite vertical porous moving plate with variable suction. *International journal of engineering science*, *38*(8), 833–845. https://doi.org/10.1016/S0020-7225(99)00063-4

[31] EL-Hakiem, M. A., Elkabeir, S. M. M., & Rashad, A. M. (n.d.). Withdrawn: Group method analysis of unsteady MHD natural convection flow over a moving vertical sheet in a fluid saturated porous medium. *Journal of computational and applied mathematics*. https://doi.org/10.1016/j.cam.2006.03.023

[32] Abd El-Naby, M. A., Elbarbary, E. M. E., & Abdelazem, N. Y. (2003). Finite difference solution of radiation effects on MHD unsteady free-convection flow over vertical plate with variable surface temperature. *Journal of applied mathematics*, *2003*(2), 380123. https://doi.org/10.1155/S1110757X0320509X

[33] Ganesan, P., & Palani, G. (2004). Finite difference analysis of unsteady natural convection MHD flow past an inclined plate with variable surface heat and mass flux. *International journal of heat and mass transfer*, *47*(19), 4449–4457. https://doi.org/10.1016/j.ijheatmasstransfer.2004.04.034

[34] Kumari, M., & Nath, G. (2006). Conjugate mixed convection transport from a moving vertical plate in a non-Newtonian fluid. *International journal of thermal sciences*, *45*(6), 607–614. https://doi.org/10.1016/j.ijthermalsci.2005.06.010

[35] Chang, C. L., & Lee, Z. Y. (2008). Free convection on a vertical plate with uniform and constant heat flux in a thermally stratified micropolar fluid. *Mechanics research communications*, *35*(6), 421–427. https://doi.org/10.1016/j.mechrescom.2008.03.007